ACR II: Improved absolute cryogenic radiometer for low background infrared calibrations

Adriaan C. Carter, Steven R. Lorentz, Timothy M. Jung, and Raju U. Datla

A second-generation absolute cryogenic radiometer (ACR II) was developed for use at the Low Background Infrared calibration facility at the National Institute of Standards and Technology. The need for spectral calibrations of very sensitive [$D^* = 10^{14}$ cm $(\mathrm{Hz})^{1/2}W^{-1}$] infrared detectors necessitated the use of a cryogenic infrared monochromator and a more sensitive radiometer. The improved low-power performance of the ACR II compared with the older absolute cryogenic radiometer (ACR) has also made it useful as the primary standard for the calibration of cryogenic blackbody sources that are used as low-power infrared sources. The responsivity of the new radiometer's receiver is 210 K/mW with a type A (random component) standard uncertainty of at most 7 pW when making power measurements of less than 10 nW. The original ACR has a responsivity of 29 K/mW and has a type A standard uncertainty of approximately 100 pW when making a similar low-noise-power measurement. Other properties of the radiometers are also described and compared.

OCIS codes: 040.3060, 040.3780, 120.3930, 120.3940, 120.4800, 120.5630.

1. Introduction

A second-generation electrical substitution radiometer has been developed as the standard detector for the spectral calibration chamber in the Low Background Infrared (LBIR) facility at the National Institute of Standards and Technology. The spectral calibration chamber is the second cryogenic vacuum system to be developed in the LBIR facility. This chamber houses a cryogenic monochromator that covers a range from 2 μm to 30 μm using selectable gratings. Calibrations performed in this chamber are typically done in a background environment having a temperature of 15 K and at a pressure of 10^{-9} Torr. The LBIR facility has been serving the infrared community for more than 10 years by providing the national standards for radiometric temperature measurements for cryogenic sources.[1] The primary standard on which the prior work was based is an older absolute cryogenic radiometer (ACR), an electrical substitution radiometer operating at a temperature of 2 K with a noise floor of 50 pW when looking at a scene with a temperature of 2 K and a maximum measurement power of 200 μm.[2] This radiometer is used primarily to measure the broadband flux emitted from blackbody sources operating over the temperature range from 150 K to 1200 K. The need for spectral measurements of infrared sources and detectors,[3] in addition to low-power broadband measurements, necessitated the development of a more sensitive radiometer.

The approach was to model the commercially available radiometer currently in use to determine which components could be optimized to improve overall performance. This was done in order to allow the continued use of the radiometer control electronics, which were not believed to be the limiting component of the system. To this end, a detailed finite-element thermal model of the ACR[4] was used to predict the effect of changes that could be made in the original design to meet the desired performance criteria. To reach our goals, higher power responsivity had to be achieved with the same level of temperature control since the same control electronics were to be used for the new receiver. In addition, the natural time constant of the cavity could not become too great; otherwise, the durations of power measurement would become impractically long. Of course, the natural time constant of the receiver is dependent on the heat

A. C. Carter (adriaan.carter@nist.gov) and R. U. Datla are with the Optical Technology Division, National Institute of Standards and Technology, 100 Bureau Drive, Mail Stop 8441, Building 221/Room B208, Gaithersburg, Maryland 20899. S. R. Lorentz (lorentz@L-1.biz) is with L-1 Standards and Technology, Inc., 10097 Tyler Place, Suite 1, Ijamsville, Maryland 21754. T. M. Jung (timothy.jung@nist.gov) is with Jung Research and Development Corporation, 1706 U Street NW, Room 204, Washington, D.C. 20009.

Received 21 June 2004; revised manuscript received 13 October 2004; accepted 14 October 2004.

0003-6935/05/060871-05$15.00/0

Table 1. Design and Performance of the Original versus the Second-Generation Absolute Cryogenic Radiometer

Receiver Cavity Property	ACR	ACR II
Apex angle of copper cone (degrees)	45	30
Receiver cone diameter (cm)	3.8	2.5
Defining aperture diameter (cm)	3	2
Estimated cavity absorptance in mid IR	0.9974	0.9993
Measured cavity absorptance at 632.8 nm	0.9987	Not measured
Copper cone thickness (μm)	127	50
Temperature sensor	Packaged GRT	Bare-chip GRT
Thermal link:		
Material	304 SS	Polyimide
Thickness (μm)	50	127
Thermal conductance at 2.2 K (W/K)	3×10^{-5}	2×10^{-6}
Heat capacity at 2.2 K (J/K)	1.5×10^{-3}	8×10^{-5}
Natural thermal time constant (s)	22	17
Responsivity at 2.2 K (K/mW)	29.7	210
Maximum power (μW)	200	100
Noise floor (pW) when enclosed in a 2 K environment	50	<8
Maximum potential thermal nonequivalence	0.0003	Not measured
(ACR)/(standard trap detector) power ratio	1.0011	1.0020
Liquid helium reservoir:		
Volume (liters)	3	15
Hold time (hours)	72	>504

capacity of the receiver and the thermal impedance of the thermal link. Increases in the impedance of the thermal link had to be accompanied by reductions in the thermal mass of the receiver cavity to keep the natural time constant from increasing.

2. Radiometer Design Improvement

The most important result of the modeling was the discovery that the stainless-steel thermal link between the heat sink and the receiver cone had 10 times the heat capacity of the copper receiver cavity when the system was at 2 K. In an ideal system, the thermal link would have zero heat capacity and would only serve as a known thermal impedance. In this case, the thermal mass of the thermal link directly contributes to the effective thermal mass of the receiver/thermal link system, thus increasing the time constant of the system. This lead to the substitution of the stainless-steel link with a link made from polyimide (Kapton)[5] in the second-generation ACR (ACR II). The heat capacity of polyimide and its thermal conductivity are both ~10 times smaller than stainless steel at 2 K.[6] The thermal link was formed from a 127-μm film of the polyimide that was rolled into a tube with one end of the tube adhered to the base of the receiver cavity cone and the other end adhered to a circular hole on the heat sink. The tubular shape of the thermal link provided very satisfactory rigidity despite the flexibility of the film when it is free standing. The dimensions of the polyimide thermal link were chosen such that its thermal impedance was approximately a factor of 10 greater than the previous stainless-steel link. The positive effect of this change is the increase in power sensitivity. An increase in time constant is normally anticipated with greater thermal impedance, except in this case the thermal mass of the thermal link that dominated the effective thermal mass of the receiver/thermal link system was reduced by approximately a factor of 10, thereby effectively eliminating this consequence.

The modeling also allowed for other beneficial changes to be made with predictable effect. Table 1 lists the major differences between the original ACR and the ACR II. The thermal mass of the receiver/thermal link system was further reduced by reducing the thermal mass of the receiver itself. This was achieved by reducing the size of the receiver cavity, thinning its walls, and replacing its packaged temperature sensor with a bare-chip version of the same sensor.

These changes to the ACR II reduced the nondriven, or natural, time constant from 22 s to 17 s, and increased the responsivity from 29.7 K/mW to 210 K/mW when the receiver cavity was operated at its lowest temperature. Improvements at the lowest temperatures are the most desirable because that is where the lowest-power measurements are made and the highest sensitivity is most desired. A typical consequence of devising an instrument with a higher responsivity is the sacrifice in the ability to make high power measurements. The ACR II only measures up to 100 μW, while the ACR measures up to 200 μW.

The model also predicts that the improvements in time response and responsivity will come with an increased nonequivalence. Nonequivalence is defined as differences in cavity temperature distributions that are caused by different heating distributions and that can result in power-measurement errors in electrical substitution radiometers, such as ACRs. One method of measuring the nonequivalence of an ACR

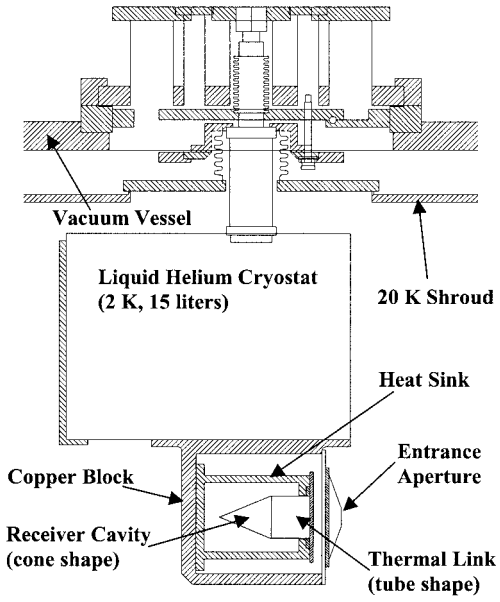

Fig. 1. Line drawing of ACR II and cryostat as it is mounted in the spectral calibration chamber.

is to place two heaters at extreme thermally nonsymmetric locations on the ACR receiver and to measure the difference in delivered heater power for a given temperature control set point between the two different heaters when operated separately. On a conical receiver cavity, such as the ACR II (Fig. 1), with the thermal link attached to the base of the cone, the two most nonsymmetric heater locations are the apex and base of the cone, and this is where the heaters are typically placed. However, for the ACR II, only one heater was used because the extra heater would have added undesirable thermal mass and another thermal leak through its leads. Thus the thermal nonequivalence was not measured for the ACR II. The goal for the ACR II was to maximize power sensitivity while maintaining a 1% expanded ($k = 3$) uncertainty. A more practical example of nonequivalence is the difference in receiver cavity heating by radiation distributed evenly on the inside of the cavity as compared with more localized resistive heating on the outside of the cavity.

The ACR model predicts two possible sources of increased thermal nonequivalence for the ACR II. First, as the thermal impedance was increased through the thermal link, the thermal leakage through the heater and temperature sensor leads became a larger fraction of the total heat dissipation. This is critical for the heaters because a fraction of the heat generated by the heater resistors can leak away without altering the temperature of the receiver cavity. This results in an electrical power measurement that is larger than the power that is actually delivered to the receiver cone. To minimize this effect on the nonequivalence, four-wire probes for each heater and sensor on the receiver were replaced with two-wire NbTi superconducting leads, which were then changed to normal four-wire leads once they were well away from the receiver. The superconducting leads are good thermal insulators, and they eliminate I^2R (Joule) heating in the leads of the heater, which also leads to power-measurement error. The other potential cause of the increased thermal nonequivalence was from the thinned walls of the receiver cavity. The increased thermal impedance through the thinner cavity walls can cause nonequivalent heating sources to have increased thermal nonequivalence. However, as a result of lessons learned from the modeling of the older ACR, the temperature sensors were placed close to the thermal link to theoretically make this problem negligible. Both of these effects exist in the ACR as well, but to a much smaller extent because of its higher-power-load design. The fraction of heat that is lost through the electrical heater leads is a smaller fraction of the heat passed through the engineered thermal link, and the wall thickness of the receiver cavity supports a smaller temperature gradient within the receiver cavity wall.

Other changes were made to improve overall system performance. A 30° receiver cone apex angle was chosen for the ACR II over the original 45° angle cone of the ACR in an effort to improve the cavity absorption. An estimate of the cavity absorption was made assuming the specular reflectance and diffuse reflectance were independent of the incidence angle and assuming a one percent diffuse reflectance for the black paint (Aeroglaze Z302, specular black)[5] that was used to coat the cavity. An absorption of 0.9993 was estimated for the ACR II as compared with 0.9974 for the ACR. We measured diffuse reflectance of Z302 to be 0.25% or less from 2 μm to 20 μm at room temperature. An absorption value of 0.9988 for the ACR was measured at the visible wavelength of 632.8 nm using an integrating sphere.[7] It is expected that the ACR II cavity has a higher absorption because, although the black paint is the same, the cavity requires more specular bounces before a ray can be reflected back out the defining aperture. Another significant change was to increase the size of the liquid He cryostat. The ACR II and its 15-l liquid He cryostat are shown in Fig. 1. The hold time of the previous cryostat was only 3 days, while the new cryostat has a hold time of greater than 3 weeks. The increased hold time is of great value because it reduces the frequency of having to refill and pump down the cryostat, which consumes an entire day of otherwise productive calibration time.

3. Results of Testing in the Low-Background-Infrared Spectral Calibration Chamber

The ACR II performed as expected and has significantly improved the calibration capabilities of the LBIR facility.[8] With the ACR II, power measurements below 100 nW are routinely made with a Type A (random component) standard uncertainty of less than 10 pW. Power measurements of 10 nW and below can be made with a Type A standard uncertainty of less than 7 pW. Figure 2 shows a 100-pW power

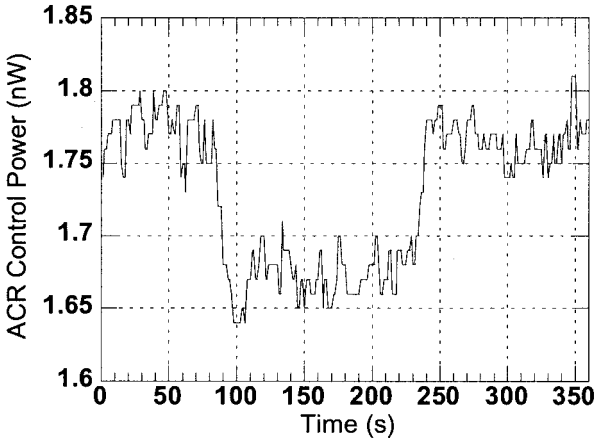

Fig. 2. 100-pW power measurement. The peak-to-peak noise is larger than the fundamental noise floor of the ACR II owing to the background noise from the scene associated with real power measurements. However, statistical analysis of these data still provides a 7-pW type A standard uncertainty.

measurement from a small defining aperture (less than 100-μm diameter) blackbody. For this measurement, the distance between the defining aperture of the blackbody and the 2-cm defining aperture of the ACR II was 30 cm. The figure shows the digitization of the electrical power delivery to the ACR II by the control electronics. The ACR II may have an intrinsic noise floor less than the measured 7 pW, but this may be masked by the effects that the control digitization has on the measured noise floor and background radiation from the surrounding environment. Clearly, significant gains in power measurement using ACRs will require an improvement in the control electronics.

A standard technique was used to make an intercomparison between the ACR II and a silicon photodiode trap detector using a 632.8-nm He–Ne laser that was actively stabilized.[2,9] The standard trap detector was directly calibrated against the absolute standard at the National Institute of Standards and Technology, the High-Accuracy Cryogenic Radiometer (HACR).[10] At laser power levels between 100 nW and 100 μW, the ACR II measured power levels that were 0.20% above those measured by the standard trap detector with a combined standard uncertainty of 0.12%. As a result, power measurements made by the ACR II are corrected by 0.20%, and the combined standard uncertainty of 0.12% of the correction is treated as a Type B (systematic component) in the uncertainty analysis. At laser powers of 100 μW and greater, the difference between the standard trap and the ACR increased abruptly to 2%, because at this power level the receiver cavity must be operated at a temperature above the superconducting critical temperature of the NbTi leads to the heaters and temperature sensors. Once the heater leads are above the critical temperature, the two-wire power measurement to the heaters is no longer accurate owing to the resistance in the leads.

During the intercomparison measurements, the spatial sensitivity of the ACR II was measured, and the optical nonuniformity was found to be negligible. For these measurements, the laser was directed toward different locations within the 2-cm defining aperture of the ACR II. The approximate 1-mm-diameter laser spot was either centered or off-center by 2.5 mm, 5.0 mm, or 7.5 mm, either vertically or horizontally for eight separate measurements. The type A standard uncertainty in all of these power measurements was 0.038%, with the largest deviation being 0.080% different from the mean. The deviations seemed to have no trend with location and were of the same order of magnitude as the power-measurement noise when measurements were repeated in the same location.

4. Summary and Future Efforts

A second-generation electrical substitution radiometer, the ACR II, was constructed that demonstrates an unprecedented noise floor for a device of this type. With a responsivity of 210 K/mW, the ACR II demonstrated a noise-floor standard deviation of 7 pW when in a 2 K environment and 7 pW type A standard uncertainty when making power measurements of less than 10 nW in a 20 K environment. The noise performance may even be better than this if it were not limited to some extent by the control electronics for the receiver cavity. In addition to greater sensitivity, the ACR II has a time constant of 17 s, and a theoretical absorption of 0.9993 in the 2 μm to 20 μm spectral region, and it only measured a 0.2% difference from the national optical power responsivity standard. Modeling of the previous ACR combined with its measured performance provided the insights that lead to the gains achieved in the ACR II design optimization and its construction. In this way, significant improvements in performance were achieved by relatively low-risk changes in design.

Efforts are in progress toward further improvements. An improvement in noise floor by a factor of ~100 while maintaining a natural time constant of less than 1 min is set as a long-term goal. The sources of nonequivalence are believed to be understood, and new design configurations will be tested to reduce the nonequivalence. Efforts to achieve these first two goals will be directed toward the reduction in overall size of the receiver cavity combined with an increased impedance of the thermal link and improvements in temperature sensor responsivity.

References and Notes

1. R. U. Datla, M. C. Croarkin, and A. C. Parr, "Cryogenic blackbody calibrations at the National Institute of Standards and Technology low background infrared calibration facility," J. Res. Natl. Inst. Stand. Technol. **99,** 77–87 (1994).
2. R. U. Datla, K. Stock, A. C. Parr, C. C. Hoyt, P. J. Miller, and P. V. Foukal, "Characterization of an absolute cryogenic radiometer as a standard detector for radiant-power measurements," Appl. Opt. **31,** 7219–7225 (1992).
3. S. R. Lorentz, S. C. Ebner, J. H. Walker, and R. U. Datla, "NIST low-background infrared spectral calibration facility," Metrologia **32,** 621–624 (1996).

4. Z. M. Zhang, R. U. Datla, S. R. Lorentz, and H. C. Tang, "Thermal modeling of absolute cryogenic radiometers," J. Heat Transfer **116,** 993–998 (1994).
5. The identification in this paper of particular commercial items does not imply endorsement by the National Institute of Standards and Technology.
6. Z. M. Zhang, S. R. Lorentz, J. P. Rice, and R. U. Datla, "Measurement of thermophysical properties for future development of cryogenic radiometers," Metrologia **35,** 511–515 (1998).
7. S. C. Ebner, A. C. Parr, and C. C. Hoyt, "Update on the low background IR calibration facility at the National Institute of Standards and Technology," in *Imaging Infrared: Scene Simulation, Modeling, and Real Image Tracking*, A. J. Huber, M. J. Triplett, and J. R. Wolverton, eds., Proc. SPIE **1110,** 49–60 (1989).
8. A. C. Carter, T. M. Jung, A. W. Smith, S. R. Lorentz, and R. Datla, "Improved broadband blackbody calibrations at NIST for low-background infrared applications," Metrologia **40,** S1–S4 (2003).
9. S. R. Lorentz and R. U. Datla, "Intercomparison between the NIST LBIR absolute cryogenic radiometer and an optical trap detector," Metrologia **30,** 341–344 (1993).
10. T. R. Gentile, J. M. Houston, J. E. Hardis, C. L. Cromer, and A. C. Parr, "National Institute of Standards and Technology high-accuracy cryogenic radiometer," Appl. Opt. **35,** 1056–1068 (1996).